

Chapter 11

Explosive Electron Emission of Carbon-Based Cathodes, and Applications



Georgiy N. Fursey

Abstract This chapter is devoted to the study of field electron (FEE) and explosive electron (EEE) emissions from carbon nanoclusters and considers the prospects of their use in the development and production of portable X-ray sources. It was found earlier that the macroscopic fields that are necessary to excite the FEE and the EEE from nanoclusters are 2–3 orders of magnitude less than those needed for conventional metal and semiconductor emitters. Recent results, related to the study of portable X-ray sources operating on the basis of explosive electron emission, are highlighted. Particular portable X-ray devices, with an explosive emission cathode made from carbon nanoclusters, are described.

11.1 Introduction

The main problem in developing portable X-ray devices stems from the necessity to apply high voltages in order to accelerate electrons to the energies required for producing bremsstrahlung, i.e., characteristic X-ray emission. This need for high voltage requires high electric insulation strength for all components used in X-ray devices. This can be difficult to achieve when high voltages are applied for long time intervals.

The problem can be solved by applying the high voltage for a very short time of the order of 10^{-9} to 10^{-7} s, i.e., by operating in the nanosecond pulsing range. The idea of constructing nanosecond-range pulsed portable X-ray devices was proposed by Tsukerman [1, 2]. In the nanosecond range, the physical linear size of a high-voltage power source could be reduced by approximately an order of magnitude, and correspondingly, the physical volume will be reduced by a factor of 10–100 times.

G. N. Fursey (✉)

The Bonch-Bruевич Saint-Petersburg, State University of Telecommunications, Saint Petersburg, Russia

e-mail: g.fursey@gmail.com

For the X-ray image (radiogram) to be registered in the nanosecond range, one needs to increase the electron flux generating the X-rays by about a million times, and this is another problem to be solved. In conventional X-ray tubes these currents are in the range 0.1–10 mA and the exposure times in X-ray diagnostics, in particular in medicine, are of the order of 0.2–1 s. To obtain a sufficient number of X-ray quanta in the nanosecond pulsing regime, one needs to increase the tube electron current to hundreds of amperes. None of the older types of electron emission (including thermionic emission) was able to provide such current values.

However, one can expect that the required emission current densities (and hence currents) could be achieved by using field electron emission (FEE). It was precisely this consideration that stimulated first Walter Dyke with coworkers [3–5], and later Tsukerman, to use field emission to obtain short X-ray pulses for studying superfast processes [6].

Tsukerman, guided by the obvious opportunities of the field emission, attempted to develop a portable X-ray apparatus. It turned out, that in the devices of Dyke [4, 7], and also those of Tsukerman [1, 6], the decisive role was played not by an ordinary field emission mechanism, but by an absolutely new phenomenon that was given the name of **explosive electron emission** (EEE) [8]. The discovery of EEE opened new frontiers for the production of nanosecond X-ray devices.

It was clear that special conditions had to be established to ensure the reproducibility of the EEE process [8, 9]. Deep understanding of how to exploit EEE cathodes made possible the production of X-ray tubes with a satisfactory service lifetime. The significant majority of the pulsed nanosecond tubes use till now refractory metal cathodes (Mo, W, etc.) [10–13].

Direct experiments have shown [14] that, during EEE, nanoscale and larger (microscale) protrusions are formed on the metal cathode surface. The “large” micrometer protrusions lead to basic erosion of the cathode surface, mass transfer in the gap, particle deposition onto the anode, and many other detrimental phenomena that affect the performance of X-ray sources.

Comparatively recently [9, 15, 16], it has been shown that carbon [8, 17] is a much more promising material for EEE cathodes, particularly when in the form of carbon nanoclusters. In many respects, they look to be much more promising devices than metal emitters.

X-ray tubes with carbon cathodes possess a high resource, ensure higher precision in the formation of the X-ray source and make possible the production of X-ray devices with an electron beam of much broader energy range, i.e., with a broader wavelength spectrum of X-ray emission than could be attained with metal cathodes.

During operation, carbon EEE cathodes produce much less contamination of the anode and other components of an X-ray tube. By using EEE from carbon materials, one can reduce the mass transfer by a factor of 10 or more. Further, in the context of particulate contamination of the anode or the exit window in a through-target X-ray tube, carbon (being a lighter material with small atomic number) absorbs a much smaller fraction of X-rays than any metal.

11.2 Experimental

11.2.1 Explosive Electron Emission (EEE)

Explosive electron emission (EEE) is a peculiar emission process that occurs when nano-sized volumes of cathode substance explode in the combined presence of a strong electrostatic surface field and the resulting high field-emission current density.

This phenomenon was discovered independently by two groups of researchers. G.N. Fursey and his coworkers studied [18] the upper limiting FEE current density and the physical mechanisms relating to vacuum breakdown and the cathode spot of a vacuum arc. The other group, headed by Mesyats [19], studied the dynamics of light emission during vacuum breakdown, using nanosecond resolution; these studies are described in detail in several publications [20–22]. A model of EEE evolution was suggested in [18] (also see [8, 9]), and was experimentally substantiated by Mesyats and coworkers [19] (see also his book [20, p. 424]).

Figure 11.1 illustrates the transition from field emission (FEE) to explosive emission (EEE), and Fig. 11.2 schematically illustrates the formation of EEE centers across the cathode surface.

Fig. 11.1 **a** Behavior of a field emission current before an explosion, for a single pointed tungsten emitter. Curves 1, 2, 3, 4, 5 and 6 are oscillograms of the FEE current as the voltage is increased; “saturation” is the transition to the saturation stage; “explosion” is the transition point to the EEE (the build-up of electron current at the instant of the explosion is shown by a dashed line). **b** Scheme (model) of the transition from field emission to explosive emission for a single point emitter

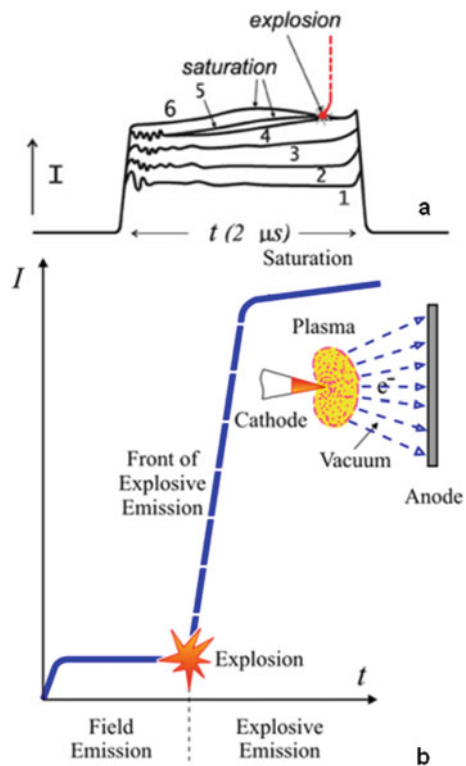
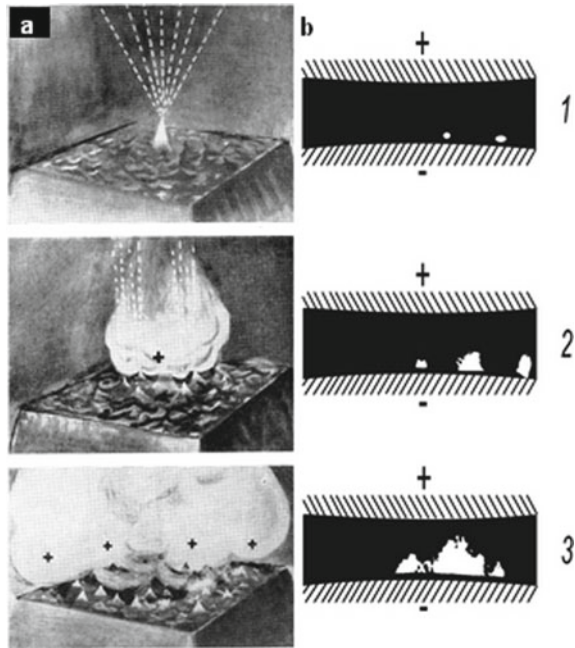


Fig. 11.2 Initiation and development of the explosive electron emission process: **a** evolution of the EEE process according to the Fursey's model; **b** diagrams 1, 2, 3 are consecutive stages of the EEE process in the direct experiments on plasma expansion, carried out by Mesyats

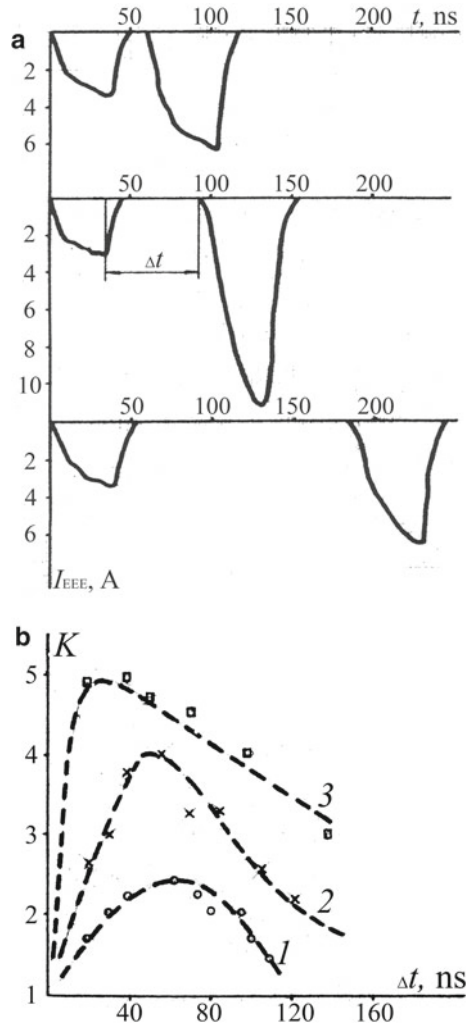


Special experiments have been carried out, using paired voltage pulses of equal amplitudes [23, 24], in order to determine the maximum frequency and minimum duty cycle needed to carry out sequential switching of the EEE current pulses. Oscillograms of the current pulses obtained at different duty cycles are shown in Fig. 11.3a. It has been found that the minimum duty cycle at which one can obtain fully identical current pulses is in the range 200–500 ns, depending on the features of the EEE cathode. Figure 11.3b shows the time dependence of the complete recovery of the EEE process. By definition, the minimum duty cycle of EEE-cathode operation is two successive nanosecond pulses [23, 24].

The process of EEE is quasi-stationary, in the sense that the conditions for EEE at the emitter surface are self-reproducing. Micro-roughness on the cathode surface is both the cause of and a result of EEE [9, 18]. In EEE, an important role is played by a liquid phase on the cathode surface. This forms as a result of the explosion of surface material and resultant heating. The liquid phase interacts with the strong electric field and with the plasma generated by the EEE, and forms nonlinear surface nano-waves: the ridges of these nano-waves then become new centers of EEE [14]. Solidification creates the micro-roughness that causes the next EEE event with the next electric field pulse.

Carbon, in this respect, possesses unique properties. It has been found that during EEE carbon also transforms into a liquid phase [14, 16, 22]. This implies that in the epicenter of the explosion the pressure may be as high as 10^4 bar (10^9 Pa).

Fig. 11.3 Experimental determination of the minimum duty cycle for adjacent FEE pulses: **a** dependence of the EEE current amplitude on pulse spacing; **b** graph illustrating the recovery of the EEE initial stage, depending on the time interval between pulses for a carbon nano-cluster cathode. The coefficient $K = I_2/I_1$ is the ratio of FEE currents in the second (I_2) and first (I_1) pulses, U_1 is the EEE excitation voltage



An advantage of a carbon-based emitter is that it is much easier to retain the nano-ridge relief on its surface, compared to metals. One can believe that, after an explosion, nano-ridges solidify not because the local cathode regions are cooling, but rather because of the pressure drop related to the process of plasma spreading. Since the pressure drops much faster than the surface cools down, after the electric field is switched off, it is possible to retain much smaller surface asperities with carbon surfaces than with metal surfaces. This ensures more uniform emission from the surface, and reduces the electric field strength required for excitation of EEE.

Table 11.1 Threshold fields F_{on} for onset of field emission. For explanation of symbols, see text

$F_{\text{on-macro}}$ (C-modif.)	$\approx 10^5\text{--}10^6$ V/m
$F_{\text{on-tip}}$ (C-modif.)	$\approx 10^7\text{--}10^8$ V/m
$F_{\text{on-tip-FEE}}$ (metals)	$\approx 3 \times 10^9$ V/m

11.2.2 Low Threshold Field and Explosive Electron Emission

In recent years one more property of carbon nanoclusters, nanotubes, and graphene has been revealed. It has been established that the excitation threshold of field emission for these materials, particularly for nanotubes and graphene, is very low. For instance, the fields at which the onset of field emission occurs were found to be 100–1000 times less than that for metals and semiconductors [9, 22, 25–30]. (For further details, see Sect. 8.6 (p. 161) in [30].) A low FEE threshold has also been detected for some other materials, for instance, diamond-like films [31].

The values of the different types of the electric field associated with the excitation of field emission (for an onset current of 10^{-10} to 10^{-9} A) are compared in Table 11.1.

In Table 11.1, $F_{\text{on-macro}}$ is the electrical field between the macroscopic electrodes with a carbon cathode; $F_{\text{on-tip}}$ is the electrical field taking into account the enhancement produced by the microtips; $F_{\text{on-tip-FEE}}$ is the local surface electrical field required for the excitation of FEE from metals.

As noted above, the main EEE excitation mechanism is the explosive destruction of local cathode areas under the action of a field emission current of very high density. Since the threshold voltage for field emission excitation is lower for the carbon nanoclusters, it follows that EEE is also excited at lower voltages.

Thus, it seems that a highly important property of a carbon nano-cluster, certainly in the context of EEE, is the formation of micro/nano-roughness (ridges) on the cathode surface. These ridges have a nano-sized radius of curvature, and this causes additional field enhancement and thus localization of emission into very small nano-sized areas of the cathode. These features provide opportunities for the development of low-voltage electron sources for EEE.

11.2.3 Development of the X-Ray Source

In the study described here, we consider two X-ray source types: a source with a tungsten needle anode (Fig. 11.4a); and a through-target source with an anode in the form of a tungsten layer coating the exit window (Fig. 11.4b).

As a cathode, we used various carbon nanoclusters, such as graphene, nanotubes, and polyacrylonitrile (PAN) fiber. Both of the designs were realized first in a special test chamber (Fig. 11.5), and then in the form of autonomous sealed-off X-ray tubes (Fig. 11.7).

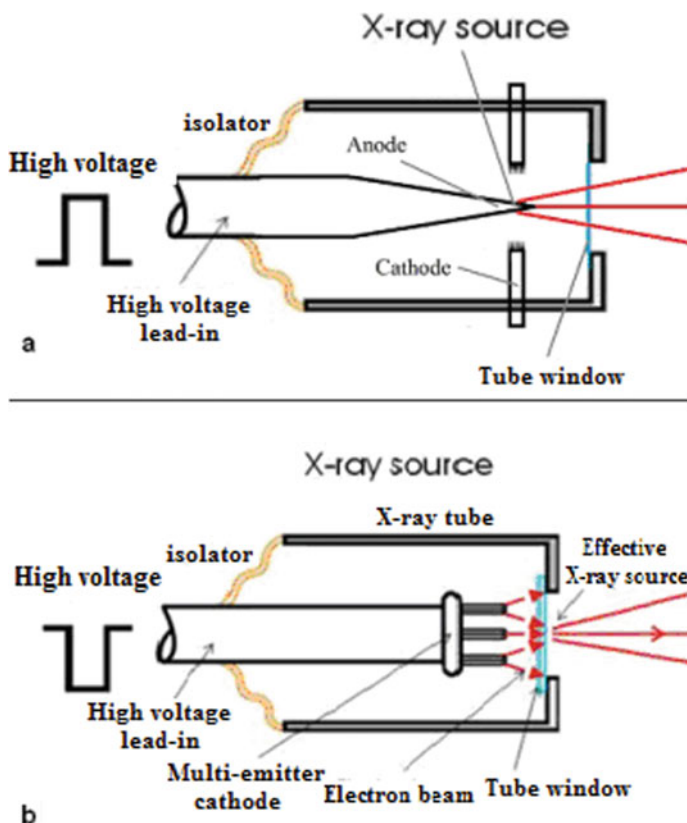


Fig. 11.4 Pulsed X-ray sources. **a** Pulsed X-ray tube with a needle anode. **b** X-ray tube with through-target anode

Fig. 11.5 Construction of the experimental chamber: 1 = high-voltage bushing; 2 = emitter; 3 = anode-grid; 4 = vacuum pumping; 5 = sorption pump; 6 = electron collector; 7 = window for photography; 8 = fluorescent screen

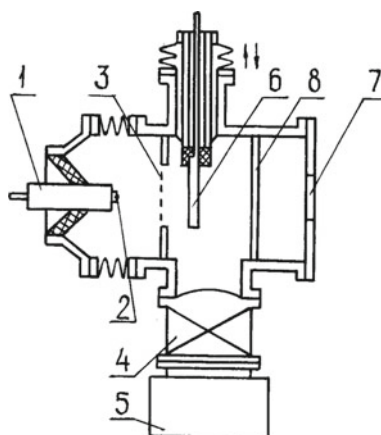
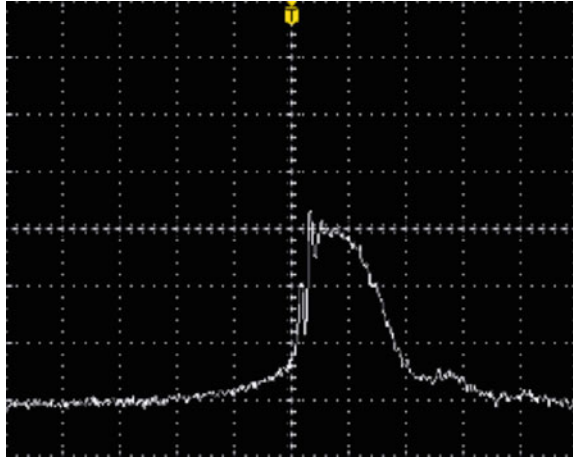


Fig. 11.6 Oscillogram of a high-voltage (75 kV) nanosecond pulse. Waveform calibration is as follows: along the horizontal axis 10 ns per division, along the vertical axis 25 kV per division



The experimental setup allows displacement of the cathode relative to the anode, using the micrometer drive, thus changing the distance between the cathode and anode. The exit window has been made of beryllium foil. A high voltage power supply is provided with special nanosecond generators.

For a dynamical study of EEE evolution, we used a generator of double (paired) nanosecond pulses [23]. We also used generators manufactured by FID Technology [32, 33].

In our experiments, the pulse duration was varied from 10 to 80 ns, and the time between double pulses from 2 to 700 ns. The pulse amplitude was in the range from 15 to 150 kV, and the pulse rise-time was 1–2 ns. A typical pulse waveform is shown in Fig. 11.6. The vacuum level in the experiments was kept at 10^{-9} to 10^{-8} Torr (10^{-7} to 10^{-6} Pa).

11.2.4 Autonomous X-Ray Tubes—Experimental Parameters of the Tubes

On the basis of the preliminary studies, we have developed and constructed experimental prototypes of autonomous sealed-off X-ray tubes (Fig. 11.7). As an anode, we took a sharpened tungsten rod with a tip radius of 0.3 mm. The exit window was made of Beryllium plate with a thickness of 400 μm to 1 mm, and the output window of the same material had a diameter of 20 mm. Vacuum in the sealed-off tube was of the order of 10^{-8} to 10^{-7} Torr (1.3×10^{-6} to 1.3×10^{-5} Pa).

The construction of our tubes was based on the standard X-ray tubes with an anticathode [11, 34]. In these tubes, a conventional metallic cathode has been replaced by a cathode made of carbon nanoclusters [17, 35].

Fig. 11.7 X-ray tube with a glass insulator



The electron current in the tube has been determined by means of a special matching coaxial shunt induced in the circuit of reverse current, and also with an oscilloscope. The electron current flowing in the diode is ultimately limited by space-charge effects, and cannot exceed the Child-Langmuir limit. With metals, the shape of a current pulse is determined by a (3/2) power law, which for a diode with a moving emission boundary [16] has the form

$$I_e(t_0) \sim \frac{U^{3/2}}{\sqrt{m_e}(d - V_{pl}t_0)^2} \quad (11.1)$$

Here U is the voltage; d is the distance between the cathode and anode; V_{pl} is the velocity of plasma expansion; and $I_e(t_0)$ is the current in the cathode-anode gap.

Maximum currents in the tube vary, in accordance with the voltage, in the range from 30 A at $U = 20$ kV, up to 200 A at $U = 75$ kV. The shape of the X-ray pulse emission was determined with the aid of a photodiode.

11.3 Results and Discussion

11.3.1 Determination of the Focal Spot Size—Divergence of the X-Ray Flux

The divergence of the X-ray beam depends on the configuration of the EEE cathode, the geometry of the gap between the cathode and the anticathode, and the geometry of the opaque (for the X-ray flux) exit section of the X-ray tube. In addition, the divergence could be varied with the aid of a special external collimator.

In our case, for the tubes with the pointed type anticathode, used in various applications, including medical ones, the divergence was about 60° . It allows the production of panoramic images with a safety margin of 40×40 cm at a standard distance of 70 cm.

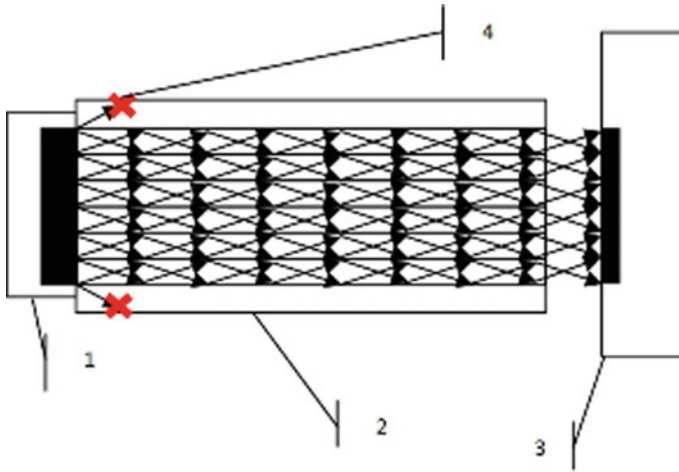


Fig. 11.8 The scheme for the transfer and determination of the X-ray spot size: 1 = an exit window of the X-ray source; 2 = poly-capillary column; 3 = visualizer for the detection of X-ray spots; 4 = the rays outside of the observation angle

The size of the X-ray spot was measured with the use of a pinhole camera [34], and in a series of experiments the poly-capillary Kumakhov pole [36] (see Fig. 11.8) was also used. In our experiments with the pointed anticathode, the minimum size of the X-ray spot was measured to be about 0.8 mm.

11.3.2 Portable X-Ray Apparatus

We have designed and produced a portable X-ray apparatus [9, 37], on the basis of the X-ray tube with a carbon cathode of PAN fiber, as developed by our group. The apparatus is shown in Fig. 11.9a, together with an anticathode. A photograph of the X-ray tube is shown in Fig. 11.9b. The summary Table 11.2 contains the basic parameters of the apparatus..

For the detection of X-ray radiation using the Radix apparatus, we explored three detector types: X-ray film, memory plates, and digital flat-panel (FP) detectors, using the indirect transformation of X-ray radiation with scintillators of sulfur oxide or gadolinium. The FP detector approach was found to be the best. At present, this type of detector is often used for digital X-ray receivers. The technology gets X-ray photons to initially interact with a scintillator; the resulting light is then transformed into an electrical signal.

For synchronization of this detector with the portable X-ray generation apparatus, a control unit with two wireless transmission line channels has been designed. It also has been used for the control of the detector: switching it off/on; controlling the

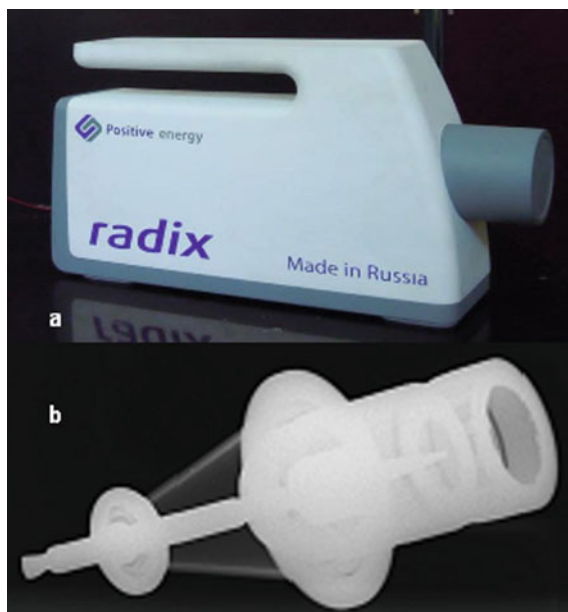


Fig. 11.9 a The portable X-ray device, and b an X-ray image of our X-ray tube

Table 11.2 Parameters of the X-ray apparatus

Accelerating voltage	15–150 kV
Beam current	50–500 A
X-ray pulse duration	10 ns
Repetition rate	up to 1000 Hz
Spot diameter	1 mm
Total weight	3 kg

regime of expectation of X-ray radiation; and managing the transfer of the digital image to a workstation display.

Control of the whole system is fully integrated by means of a developed software suite called “Radix Center”. This is able to operate the X-ray generator and detectors, and carry out various supporting tasks, including pre- and post-treatment of the images, calibration of the detector, and system optimization (for example, to minimize the noise level and reduce the number of artifacts, such as faulty pixels).

Various X-ray images obtained with our portable apparatus are shown in Figs. 11.10–11.16.

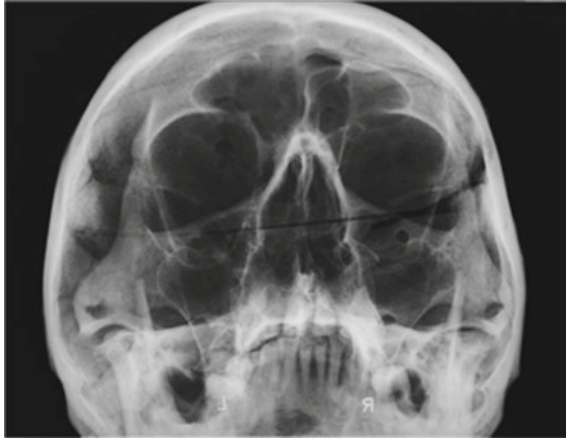


Fig. 11.10 Radiograph of a human skull



Fig. 11.11 X-ray image of a human hand

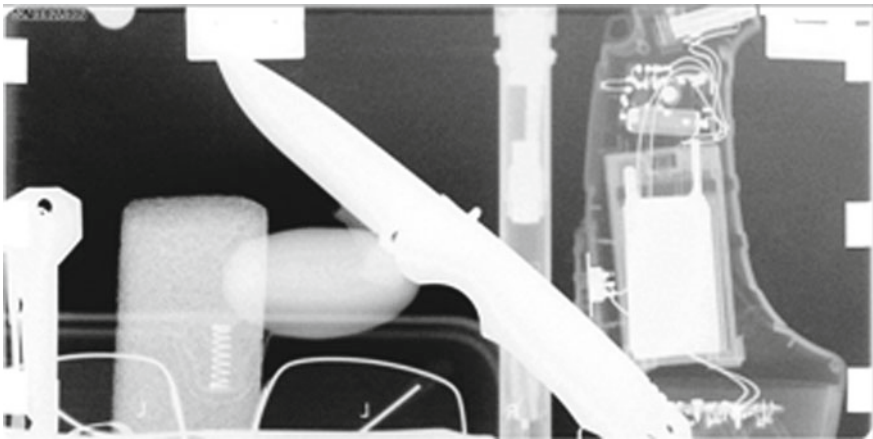
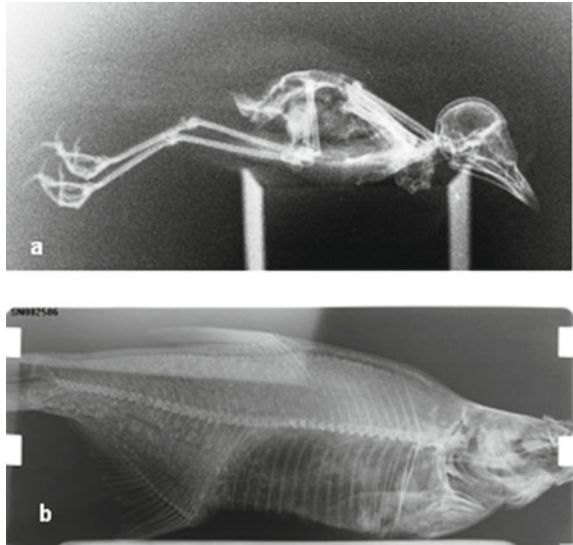
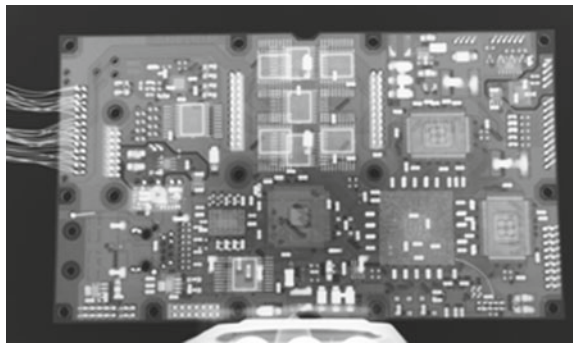


Fig. 11.12 Inside of a briefcase

Fig. 11.13 a Bird and b fish**Fig. 11.14** Circuit board

11.3.3 Opportunities for External Focusing of Pulsed X-Ray Radiation

The main obstacle affecting the quality of our X-ray images is the comparatively large size of the X-ray spot (1–2 mm). In pulsed X-ray tubes operated using EEE, reduction of the spot by means of internal electromagnetic focusing is troublesome, because of the small distance between cathode and anode. A more attractive approach is direct focusing of the X-ray radiation after exit from the X-ray tube. This seems to be possible in principle, by using the poly-capillary X-ray optics proposed by Kumakhov [38–40] (in particular, see pp. 170–182 in [38]). As shown in a number of recent studies, the Kumakhov lens in principle allows X-ray focusing on a spot with a diameter of less than 6 μm .

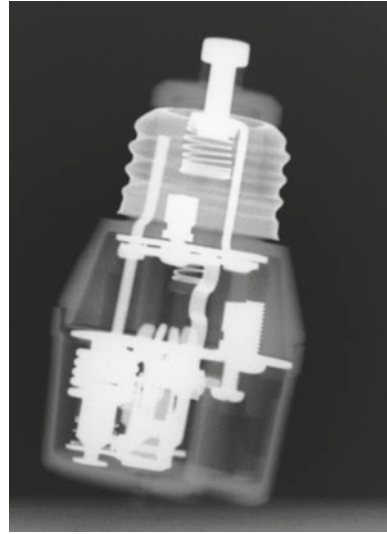
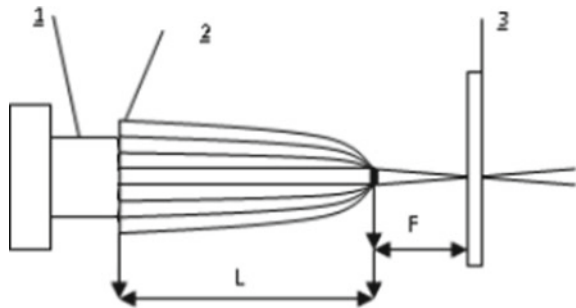
Fig. 11.15 Automatic fuse

Fig. 11.16 The principle of external focusing: 1 = head part of X-ray tube; 2 = poly-capillary half-lens; 3 = visualizer; focal length $F = 160$ mm, and lens length $L = 268$ mm. Diameter of the half-lens inlet is 11.3 mm. Diameter of the half-lens outlet is 6 mm



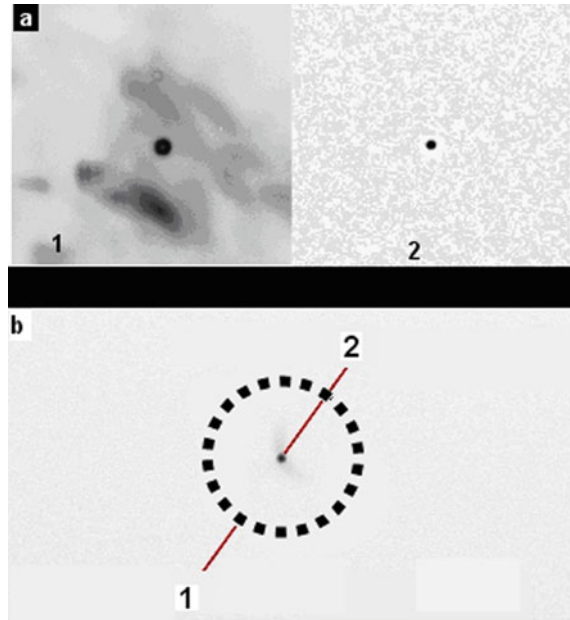
Efficient performance of these lenses has been achieved in a number of devices with stationary X-ray sources.

This study, continuing our previous experiments, now reports attempts [41] to apply this kind of optics to our powerful pulsed X-ray sources driven by EEE in the nanosecond range.

The principle of external focusing rests on the phenomenon of total external reflection. In the X-ray spectral range, the refractive index $n < 1$ because a vacuum is optically the more dense medium. The reflection property is highest at glancing angles of incidence. Figure 11.16 shows the principal scheme of focusing by the aid of poly-capillary optics.

Some results of our studies are now given. Two experiments were carried out. In the first we used the X-ray source (X-ray tube) with a pointed (needle) anticathode (= anode). In this case, we managed to compress the X-ray spot by a factor of approximately 2 (see Fig. 11.17a). In the second, the experiment was carried out

Fig. 11.17 Results of X-ray focusing with the aid of a Kumakhov half-lens. **a** The X-ray spot obtained with the X-ray tube using a pointed anti-cathode: 1 = the central black spot is the original X-ray spot; 2 = the focused X-ray spot. **b** X-ray spot obtained with the through-target X-ray tube: 1 = dotted circle outlines the original X-ray spot; 2 = the focused X-ray spot



with the through-target X-ray tube. Here, the entry orifice of the external half-lens was placed directly at the tube exit window. The diameter of the X-ray spot on the window was 11 mm, and was approximately equal to the diameter of the entrance to the capillary half-lens. On exit from the capillary half-lens, the spot diameter was measured to be 0.5 mm (see Fig. 11.17b).

The results obtained from these experiments show that the external focusing of pulsed X-ray sources seems to have considerable promise.

11.4 Summary and Conclusions

The results reported in the chapter can be summarized as follows:

1. We have briefly analyzed the mechanism of explosive electron emission (EEE) from a viewpoint of contemporary understanding of this phenomenon.
2. The special features of EEE, when it occurs from carbon nanoclusters, have been discussed.
3. X-ray tubes, developed on the basis of EEE from carbon nanoclusters, have been thoroughly studied.
4. A new family of portable pulsed X-ray tubes has been proposed; these have attractive potential applications.
5. It was shown, that the external focusing of X-ray radiation in pulse mode is perspective.

In conclusion, I would like to mention that the community of scientists engaged in the development of portable X-ray instrumentation is quite numerous. I would especially like to recognize the studies performed by Komyak, Mesyats, Peliks, and Belkin [10, 13].

Acknowledgements The author and his coworkers are glad to express their deep gratitude to B.P. Merkulov for his generous offer to use his ceramic X-ray tube to carry out our studies of EEE cathodes, and to Prof. Aleksina for the opportunity to test our apparatus in the Anatomic museum of the Saint-Petersburg First Medical University. We are indebted to the Head of the Firm “Spectroflash”, Dr. E.A. Peliks, for fruitful discussions, and also to the Firm “Positive Energy” for comprehensive support of the research described. We offer special thanks to D.N. Fomin for his valuable technical assistance. The author is also grateful to Dr. Richard G. Forbes for critical reading of the manuscript.

References

1. V.A. Tsukerman, L.V. Tarasova, S.I. Lobov, New sources of X rays. *Sov. Phys. Uspekhi* **14**, 61–71 (1971)
2. V.A. Tsukerman, Portable sources of X-ray beams, *Vestnik AN USSR* **1971**(11), 18–25 (1971). (in Russian)
3. W.P. Dyke, J.P. Barbour, F.J. Grundhauser, VII Int. Congr. Kurzzeitphotogr. Zurich, Switzerland (1965)
4. W.P. Dyke, Advances in field emission. *Sci. Am.* **210**(1), 108–118 (1964)
5. F.G. Grundhauser, W.P. Dyke, S.D. Bennet, A fifty-milli-microsecond flash X-ray system for high-speed radiographs. *J. SMPTE* **70**, 435–439 (1961)
6. V.A. Tsukerman, M.A. Manakova, Short X-ray flash sources for investigating fast processes. *Zh. Tekh. Fiz.* **27**, 391–403 (1957). (in Russian)
7. W.P. Dyke, W.W. Dolan, Field emission. *Adv. Electron. Electron Phys.* **8**, 89–185 (Academic, New York, 1956)
8. G.N. Fursey, Field emission in microelectronics, in: *Field Ion and Field Electron Microscopy and Spectroscopy: History, Achievements, the Current State of the Art, and Prospects*, ed. by A.L. Suvorov (Akademprint, Moscow, 2003), pp. 170–189. (in Russian)
9. G.N. Fursey, Intensive electron emission in a strong electric fields in vacuum microelectronics and high-power electronics. *Nanotechnol. Percept.* **9**, 167–185 (2013)
10. E.A. Pelix, X-ray pulse apparatus based on explosive electron emission, in 17th World Conference on Nondestructive Testing, Shanghai, China, October 2008
11. G.V. Melnichuk, B.P. Merkulov, D.S. Makhanko, V.G. Samorodov, Development of pulsed metal-ceramic explosive emission tubes with improved X-ray technical characteristics, defense industry achievements. *Russ. Sci. Tech. Prog.* **2014**(2), 53–67 (2014)
12. G.N. Fursey, E.A. Pelix, The new generation of medical x-ray discrete instrumentation. *Pract. High Power Electron.* **44**, 47–51 (2011)
13. A.A. Altuhov, N.V. Belkin et al., High power pulse X-ray apparatus, “Kavkaz” for non-destructive control. *Defectoscopyia* **11**, 12–17 (1989). (in Russian)
14. G.N. Fursey, L.A. Shirochin, L.M. Baskin, Field emission processes from liquid-metal surface. *J. Vac. Sci. Technol. B* **15**, 410–421 (1997)
15. G.N. Fursey, M.A. Polyakov, A.A. Kantonistov, A.M. Yafyasov, B.S. Pavlov, V. B. Bozhevov’nov, Field and explosive emissions from graphene-like structures. *Tech. Phys.* **58**, 845–851 (2013)
16. G.A. Mesyats, D.I. Proskurovsky, *Pulsed Electrical Discharge in Vacuum* (Springer, Berlin, 1989)

17. G.N. Fursey, L.A. Shirochin, P.N. Bespalov, X-ray tube. Patent of Russian Federation No 2308781, Bull. No. 29 (20 October 2007)
18. G.N. Fursey, P.N. Vorontsov-Vel'yaminov, A qualitative model of vacuum arc initiation. *Zh. Tech. Fiz.* **37**, 1870–1888 (1967). (in Russian)
19. S.P. Bugaev, A.M. Iskol'ski, G.A. Mesyats, D.I. Proskurovskii, Electron-optical observation of initiation and development of pulsed breakdown of short vacuum gap. *Zh. Tech. Fiz.* **37**, 2206–2208 (1967). (in Russian)
20. G.A. Mesyats, *Cathode Phenomena in a Vacuum Discharge: The Breakdown, the Spark, and the Arc* (Nauka, Moscow, 2000)
21. G.A. Mesyats, G.N. Fursey, Explosive field emission at the initial stages of vacuum discharge, in *Cold Cathodes*, ed. by M.I. Elinson (Sovetskoe Radio, Moscow 1974). (in Russian)
22. G.N. Fursey, Field emission in vacuum microelectronics. *Appl. Surf. Sci.* **215**, 113–134 (2003)
23. B.I. Grishanov, L.A. Shirochin, G.N. Fursey, S.M. Lupekhin, M.A. Polyakov, V.M. Zhukov, High-voltage generator of variable nanosecond pulses for study of explosive electron emission. *Instrum. Exp. Tech.* **29**, 851–854 (1987)
24. G.N. Fursey, C.M. Lupekhin, M.A. Polyakov, L.M. Baskin, L.A. Shirochin, Dynamics of explosive emission processes. *Doklady Akademii Nauk (DAN) USSR*, **276**, 866–869 (1984). (in Russian)
25. G.N. Fursey, *Field Emission in Vacuum Microelectronics* (Kluwer Academic/Plenum, New York, 2005)
26. N.I. Sinit'syn, Yu.V. Gulyaev, N.D. Devjatkov et al., Carbon nanocluster structures as one of materials of emission electronics in the future. *Radiotekhnika* **2(9)** (2000). (in Russian)
27. A.N. Obratsov, Dual-barrier tunneling during field emission from nano-graphite, in Joint Conference IVESC-ICEE-ICCTPEA-BDO-2014, Saint-Petersburg, Russia (30 June–04 July 2014)
28. A.I.A. Zakhidov, A.N. Obratsov, A.P. Volkov, DA. Lyashenko, Mechanism of low-voltage field emission from nanocarbon materials. *J. Exp. Theor. Phys.* **100**, 89–94 (2005)
29. A.N. Obratsov, IYu. Pavlovsky, A.P. Volkov, Low-voltage electron emission from chemical vapor deposition graphite films. *J. Vac. Sci. Technol., B* **17**, 674–678 (1999)
30. A. Yafyasov, V. Bogevolnov, G. Fursey, B. Pavlov, M. Polyakov, A. Ibragimov, Low-threshold field emission from carbon nano-clusters. *Ultramicroscopy* **111**, 409–414 (2011)
31. A.T. Rakhimov, V.A. Samorodov, E.S. Soldatov et al., Study of emission and structure characteristic correlation of diamond films by scanning tunneling microscopy. *Poverkhnost* **7**, 47 (1999). (in Russian)
32. V. Efanov, M. Efanov, Gigawatt all solid state FID pulsers with nanosecond pulse duration, in Proceedings of IEEE International Power Modulators and High Voltage Conference, Las Vegas, May 2008, p. 381
33. V.M. Efanov, P.M. Yarin, A.V. Kricklenko, V.A. Mankevich, High voltage nanosecond pulsers for plasma chemistry and gas discharge, in Proceedings 2008 IEEE International Power Modulators and High Voltage Conference, Las Vegas, USA, May 2008 (ISBN-978-1-4244-1534-2) (IEEE, Piscataway, 2008), pp. 178–180
34. M.A. Polyakov, G.N. Fursey, L.A. Shirochin, A.A. Kantonistov, An X-ray technique for investigation of the explosive-emission cathode surface. *Tech. Phys. Lett.* **34**, 586–587 (2008)
35. B.P. Merkulov, G.N. Fursey, D.S. Makhan'ko, M.A. Poljakov, Pulse type X-ray tube, Patent of Russian Federation No 2308781, Bull. No. 18 (27.06.2014). (in Russian)
36. A.A. Kumakhov, I.V. Dmitriev, Methods of measuring X-ray sources and neutron radiation using poly-capillary optics. *J. Appl. Phys.* **81**, 85–87 (2011)
37. L.A. Shirochin, G.N. Fursey, High-power soft X-ray tube with an explosive emission cathode. In: Proceedings of XVIII International Symposium on Discharges and Electrical Insulations in Vacuum, Eindhoven, Netherlands, August 1998, pp. 672–674
38. M.A. Kumakhov (ed.), Proceedings of International Conference on X-ray and Neutron Capillary Optics, Zvenigorod, Russian Federation, September 2001, SPIE Vol. 4765
39. V.A. Arkadiev, D.I. Gruev, M.A. Kumakhov, X-ray lens for forming quasisparallel beam, in *Optics of Beams*, ed. by M.A. Kumakhov (IROS, Moscow, 1993), pp. 27–32

40. G.I. Borisov, M.A. Kumakhov, Poly-capillary lens for neutrons. Nucl. Instr. Meth. Phys. Res. A **529**, 129–133 (2004)
41. G.N. Fursey, I.A. Dmitriev, Y.B. Skuratnik, A.A. Begidov, A.A. Kumakhov, Focusing possibility of high-power nanosecond X-ray pulses. Prakticheskaya silovaya elektronika **2**(46), 50–55 (2012). (in Russian)